BIOCHEMISTRY
including biophysical chemistry & molecular biology
Article

Biochemistry **2009,** *48,* 5303–5312 5303
DOI: 10.1021/bi9004705

Elucidation of the Molecular Basis of Cholecystokinin Peptide Docking to Its Receptor Using Site-Specific Intrinsic Photoaffinity Labeling and Molecular Modeling[†]

Maoqing Dong,[‡] Polo C.-H. Lam,[§] Delia I. Pinon,[‡] Ruben Abagyan,[§] and Laurence J. Miller*,[‡]

[‡]*Department of Molecular Pharmacology and Experimental Therapeutics, Mayo Clinic, Scottsdale, Arizona 85259, and* [§]*Department of Molecular Biology, Scripps Research Institute and Molsoft LLC, La Jolla, California 92037*

Received March 18, 2009; Revised Manuscript Received April 22, 2009

ABSTRACT: G protein-coupled receptors represent the largest family of receptors and the major target of current drug development efforts. Understanding of the mechanisms of ligand binding and activation of these receptors remains limited, despite recent advances in structural determination of family members. This work focuses on the use of photoaffinity labeling and molecular modeling to elucidate the structural basis of binding a natural peptide ligand to a family A G protein-coupled receptor, the type 1 cholecystokinin receptor. Two photolabile cholecystokinin analogues were developed and characterized as representing high-affinity, fully biologically active probes with sites of covalent attachment at positions 28 and 31. The sites of receptor labeling were identified by purification, proteolytic peptide mapping, and radiochemical sequencing of labeled wild-type and mutant cholecystokinin receptors. The position 28 probe labeled second extracellular loop residue Leu^{199}, while the position 31 probe labeled first extracellular loop residue Phe^{107}. Along with five additional spatial approximation constraints coming from previous photoaffinity labeling studies and 12 distance restraints from fluorescence resonance energy transfer studies, these were built into two homology models of the cholecystokinin receptor, based on the recent crystal structures of the β2-adrenergic receptor and A2a-adenosine receptor. The resultant agonist ligand-occupied receptor models fully accommodate all existing experimental data and represent the best refined models of a peptide hormone receptor in this important family.

There has been substantial recent progress in our understanding of the structure of receptors of family A guanine nucleotide-binding protein (G protein)-coupled receptors (GPCRs),[1] with the recent success being crystallization of the β2-adrenergic receptor, the β1-adrenergic receptor, the A2a-adenosine receptor, and opsin (*1*−*4*). The type 1 cholecystokinin (CCK) receptor is prototypic of the group of receptors in this family that bind and are activated by natural peptide hormones and neurotransmitters. Like many peptides that bind to members of this family of receptors, the critical region of the CCK ligand is within a focused region of its carboxyl terminus. For CCK, this pharmacophoric domain represents the carboxyl-terminal heptapeptide-amide (CCK-27−33) (*5*). Remarkably, site-specific intrinsic photoaffinity labeling studies have been performed for five residues spread throughout and immediately adjacent to this region, with experimentally derived constraints utilized to establish working models of the agonist-occupied receptor that were based on the rhodopsin structure (*6*), representing the best template then available (*7*−*11*). However, this model is quite distinct from another working model that has been proposed for the CCK−receptor complex that is based largely on mutagenesis data (*12*).

In this work, our goal was to enhance our understanding of the peptide-occupied CCK receptor, utilizing the recently described crystal structures of the β2-adrenergic receptor (*1*) and the A2a-adenosine receptor (*2*) as structural templates for initial modeling potentially better than rhodopsin (*6*) and refining these structures by adding experimentally defined constraints. We have developed two new CCK analogues that represent intrinsic photoaffinity labeling probes for this receptor, characterized them as full agonists, and utilized them to identify the specific receptor residues that they were able to covalently label after docking. These new spatial approximation constraints were then utilized along with all existing experimentally derived constraints to develop new three-dimensional molecular models of the CCK−receptor complex. While these models are most similar to the previous photoaffinity labeling model built on the basis of homology with rhodopsin (*8*) and quite distinct from the previous model of the CCK receptor based on mutagenesis data (*12*), there are substantial improvements in structural insights that have

[†]This work was supported by Grant DK32878 from the National Institutes of Health, grants from the Fiterman Foundation, and the Mayo Clinic.

*To whom correspondence should be addressed: Mayo Clinic, 13400 E. Shea Blvd., Scottsdale, AZ 85259. Telephone: (480) 301-6650. Fax: (480) 301-6969. E-mail: miller@mayo.edu.

[1]Abbreviations: (BzBz)Lys, *p*-benzoylbenzoyl-L-lysine; CCK, cholecystokinin; CHO-CCKR, rat type 1 CCK receptor-bearing Chinese hamster ovary cell line; CNBr, cyanogen bromide; ECL, extracellular loop; GPCR, G protein-coupled receptor; FRET, fluorescence resonance energy transfer; KRH, Krebs-Ringer/HEPES; ICM, Internal Coordinate Mechanics; TM, transmembrane domain.

© 2009 American Chemical Society Published on Web 04/29/2009

come from the new receptor templates and the additional spatial approximation constraints. This provides still further insight into the molecular basis for peptide binding and activation of a family A GPCR.

MATERIALS AND METHODS

Materials. Cholecystokinin octapeptide (CCK-26−33, with the numbering based on the 33-amino acid form of this hormone first isolated and characterized) was purchased from Bachem (Torrance, CA). Cyanogen bromide (CNBr), the solid-phase oxidant, *N*-chlorobenzenesulfonamide (Iodobeads), and *m*-maleimidobenzoyl-*N*-hydroxysulfosuccinimide ester were purchased from Pierce Chemical Co. (Rockford, IL). 3-Isobutyl-1-methylxanthine and *N*-(2-aminoethyl-1)-3-aminopropyl glass beads were from Sigma (St. Louis, MO). Endoproteinase Lys-C was from Roche Applied Science (Indianapolis, IN). Soybean trypsin inhibitor and tissue culture medium were from Gibco (Grand Island, NY). Endoglycosidase F was prepared in our laboratory, as we have described previously (*13*). All other reagents were of analytical grade.

Synthetic Peptides. The photolabile CCK probes used in this work were des-amino-Tyr-Gly-[((BzBz)Lys^{28},Nle^{31})CCK-26−33] [(BzBz)Lys^{28} probe] and des-amino-Tyr-Gly-[(Nle^{28},(BzBz)Lys^{31}) CCK-26−33] [(BzBz)Lys^{31} probe] (Figure 1). They were designed to incorporate a photolabile *p*-benzoylbenzoyl-L-lysine in position 28 or 31 to replace each of the Met residues individually. The Met residue at position 31 for the (BzBz)Lys^{28} probe and at position 28 for the (BzBz)Lys^{31} probe was replaced with oxidation-resistant norleucine (Nle) residues. Each peptide also had an amino-terminal extension of Tyr-Gly to provide a site for oxidative radioiodination. Each probe had its amino terminus blocked by using a des-amino-tyrosine to permit radiochemical sequencing of the labeled receptor fragments without concomitant probe cleavage during cycles of Edman degradation. These modifications were tolerated well as we demonstrated previously (*11*). Both peptides were synthesized as we have described previously (*14*), radioiodinated using the solid-phase oxidant, Iodobeads, and purified to homogeneity using reversed-phase HPLC to yield specific radioactivities of 2000 Ci/mmol.

Receptor Preparations. Receptor resources included Chinese hamster ovary (CHO) cell lines stably expressing the wild-type rat type 1 CCK receptor (CHO-CCKR) (*15*) and L104M (*7*), M195L (*16*), A204C (*17*), and V342M (*10*) mutant CCK receptors. They were cultured at 37 °C in a 5% CO_2 environment on Falcon tissue culture plasticware in Ham's F-12 medium supplemented with 5% Fetal Clone-2 (HyClone Laboratories, Logan, UT). Cells were passaged twice a week and lifted mechanically before use. Plasma membranes were prepared using discontinuous sucrose gradient centrifugation (*15*). Membranes were then resuspended in Krebs-Ringers/HEPES (KRH) medium containing 25 mM HEPES (pH 7.4), 104 mM NaCl, 5 mM KCl, 2 mM $CaCl_2$, 1 mM KH_2PO_4, 1.2 mM $MgSO_4$, 0.01% soybean trypsin inhibitor, and 1 mM phenylmethanesulfonyl fluoride for storage at −80 °C until they were to be used.

In addition, it was necessary to generate a new CCK receptor mutant that eliminated a naturally occurring site for CNBr cleavage in the second extracellular loop of the receptor. This represented a Met^{205} to leucine (M205L) receptor construct. It was prepared using an oligonucleotide-directed approach with the QuikChange site-directed mutagenesis kit from Stratagene (La Jolla, CA) with its sequence verified by direct DNA sequencing. This receptor mutant was expressed transiently in COS-1 cells (American type Culture Collection, Manassas, VA) after transfection using a modification of the DEAE-dextran method (*18*). Cells were maintained under the same conditions as the CHO cells described above, except the culture medium was Dulbecco's modified Eagle's medium supplemented with 5% Fetal Clone-2. Forty-eight hours after transfection, cells were used either directly in binding and biological activity studies or for membrane preparation for photoaffinity labeling studies.

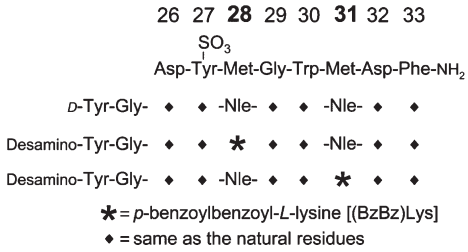

FIGURE 1: Primary structures of CCK analogues used in this work. Shown are the sequences of the natural peptide agonist, CCK-26−33 (top line with residue numbers above), the radioligand used in binding assays, D-Tyr-Gly-[(Nle^{28,31})CCK-26−33] (line 2), and the probes incorporating a photolabile residue, *p*-benzoylbenzoyl-L-lysine, into positions 28 and 31, respectively, (BzBz)Lys^{28} probe (line 3) and (BzBz)Lys^{31} probe (line 4).

Binding Studies. The (BzBz)Lys^{28} and (BzBz)Lys^{31} probes were characterized for their binding activities using enriched plasma membranes from the CHO-CCKR cells in standard competition binding assays, using conditions that have been previously established (*15*). In brief, membranes (containing approximately 10 μg of protein) were incubated with a constant amount of radioligand, ^{125}I-D-Tyr-Gly-[(Nle^{28,31})CCK-26−33] (5−10 pM), and increasing concentrations of nonradioactive ligand [0−1 μM (BzBz)Lys^{28} or (BzBz)Lys^{31} probe] in KRH medium containing 0.2% bovine serum albumin for 1 h at room temperature (final volume of 500 μL). Separation of bound from free radioligand was performed with a Skatron cell harvester (Molecular Devices, Sunnyvale, CA), using receptor binding filtermats. Bound radioactivity was quantified using a γ-spectrometer. Nonspecific binding was assessed in the presence of 1 μM unlabeled CCK and represented less than 15% of the total binding. Data were graphed using Prism (GraphPad Software, San Diego, CA) and were analyzed using the nonlinear least-squares curve-fitting program, LIGAND (*19*).

Biological Activity Assay. The biological activities of the (BzBz)Lys^{28} and (BzBz)Lys^{31} probes were studied using assays for stimulation of intracellular calcium in CHO-CCKR cells as we have previously described (*15*). In brief, cells were lifted with nonenzymatic cell dissociation solution (Sigma), washed, and loaded with 5 μM Fura-2 acetoxymethyl ester in serum-free culture medium at 37 °C for 20 min. After being washed with KRH medium twice, approximately 2 million cells per assay were stimulated with varied concentrations of CCK or (BzBz)Lys^{28} or (BzBz)Lys^{31} probe at 37 °C, with fluorescence quantified in a Perkin-Elmer (Norwalk, CT) LS50B luminescence spectrometer. Excitation was performed at 340 and 380 nm, and emissions were determined at 520 nm, with calcium concentrations calculated from the ratios as described by Grynkiewicz et al. (*20*). The peak intracellular calcium transients were utilized to determine the concentration dependence of the biological responses. Basal levels of calcium were measured in the absence of agonist stimulation, whereas maximum levels were determined as the

Table 1: C_β−C_β Distances between Cross-Linked Residues in the Best Models

CCK peptide residue	CCK receptor residue	β2-adrenergic receptor-based model (Å)	A2a-adenosine receptor-based model (Å)
Asp^{24}	Glu^{345}	8.1	8.2
$Tyr^{27}(SO_3)$[a]	Arg^{197}	5.0	4.1
Nle^{28}	Leu^{199}	7.5	7.5
Gly^{29}[b]	His^{347}	8.3	8.4
Gly^{29}[c]	Leu^{348}	7.4	7.3
Trp^{30}	Leu^{99}	12.1	11.6
Nle^{31}	Phe^{107}	8.3	8.0
Phe^{33}	Trp^{39}	8.2	8.3

[a] Measured between the sulfur atom of Tyr^{27} and C_ζ of Arg^{197}. [b] Measured between $H_{\alpha1}$ of Gly^{29} and C_β of His^{347}. [c] Measured between $H_{\alpha2}$ of Gly^{29} and C_β of Leu^{348}.

peak intracellular calcium concentrations measured in the presence of 1 μM CCK. Stimulated values were calculated as percentages of the range of calcium concentrations between basal and maximal levels. All assays were performed in duplicate and repeated at least three times in independent experiments. This assay was also used to characterize the biological activity of the new receptor mutant (M205L) that was transiently expressed in COS-1 cells.

Photoaffinity Labeling. This was performed by incubation of 0.1 nM radioiodinated (BzBz)Lys^{28} or (BzBz)Lys^{31} probe with 50 μg of CHO-CCKR membranes in the dark at 25 °C for 1 h in KRH medium in the absence and presence of increasing concentrations of competing CCK (from 10^{-10} to 10^{-6} M). Photolysis was performed in a Rayonet Photochemical Reactor (Southern New England Ultraviolet, Hamden, CT) equipped with 3500 Å lamps at 4 °C for 30 min. Membranes were then washed, solubilized with 1% Nonidet P-40 in KRH medium, and purified by wheat germ agglutinin−agarose affinity chromatography prior to SDS−polyacrylamide gel electrophoresis (*21*). The affinity-labeled receptor was visualized by autoradiography. The apparent molecular masses of radiolabeled receptors were determined by interpolation on plots of the mobility of ProSieve protein standards (Lonza Rockland, Inc., Rockland, ME) versus the log values of their apparent masses.

Peptide Mapping. Chemical and enzymatic cleavage of the wild-type receptor were used to localize the domains of labeling with the (BzBz)Lys^{28} and (BzBz)Lys^{31} probes. This required a larger-scale preparation of photoaffinity-labeled receptor. For this, approximately 200 μg of CHO-CCKR membranes was incubated with 0.5 nM radioiodinated (BzBz)Lys^{28} or (BzBz)-Lys^{31} probe in the absence of competing CCK prior to photolysis and electrophoresis.

Radiolabeled receptor was gel-purified to radioactive homogeneity and cleaved with CNBr and endoproteinase Lys-C using procedures we have previously described in detail (*22*). The products of cleavage were resolved on 10% NuPAGE gels with MES running buffer (Invitrogen, Carlsbad, CA), with labeled fragments visualized by autoradiography. The apparent molecular masses of radiolabeled receptor fragments were determined by interpolation on a plot of the mobility of Multimark protein standards (Invitrogen) versus the log values of their apparent masses. For selected experiments, gel-purified labeled receptor and its relevant fragments were deglycosylated with endoglycosidase F using conditions we have described previously (*15*).

Radiochemical Sequencing. After achieving definitive identification of the receptor fragments labeled with each probe, we used radiochemical Edman degradation sequencing to determine the specific sites of attachment (*23*). For the (BzBz)Lys^{28} probe, we used the A204C CCK receptor mutant, and for the (BzBz)-Lys^{31} probe, we used both wild-type and L104M mutant CCK receptor. Labeled receptor was purified and cleaved by CNBr, and the resultant fragments were gel-purified to radioactive homogeneity and covalently coupled through their cysteine residues (Cys^{204} or Cys^{114}) to maleimidobenzoyl succinimide-activated *N*-(2-aminoethyl-1)-3-aminopropyl glass beads. Repetitive cycles of manual Edman degradation were then performed with quantitation of radioactivity released in each cycle. This procedure was repeated three times in independent experiments.

Molecular Modeling. All molecular modeling activities for this project were conducted utilizing a stochastic global energy optimization procedure that has been implemented in Internal Coordinate Mechanics (ICM) (*24*). This procedure consisted of three iterative steps: (a) random conformational change of a dihedral angle according to the biased-probability Monte Carlo method (*25*), (b) local minimization of all free dihedral angles, and (c) acceptance or rejection of the new conformation based on the Metropolis criterion at the simulation temperature, usually at 600 K (*26*). This approach can generate and search through diverse sets of molecular conformations by actively sampling a selected set of dihedral angles. All calculations were conducted on 2.33 GHz Intel dual-core XEON-EMT processors.

To build a model of the transmembrane helical bundle domain of the CCK receptor, we used the multiple-sequence alignment of family A GPCRs at the PROSITE database as a reference (*27*). The previously described transmembrane bundle and loop modeling method was used (*28*) with the crystal structures of the human β2-adrenergic receptor and the A2a-adenosine receptor as templates for two independent modeling simulations (*1*, *2*). After initial simulations, full atomic models of the transmembrane domains were constructed by connecting the helical bundle regions with the loops in one continuous chain.

The experimentally determined structure of CCK-26−33 was used as a template to construct the decapeptide Asp^{24}-Arg^{25}-Asp^{26}-$Tyr^{27}(SO_3)$-Nle^{28}-Gly^{29}-Trp^{30}-Nle^{31}-Asp^{32}-Phe^{33}-NH_2 (CCK-24−33) used in the simulation (*29*). Eight distance restraints were set between CCK peptide residues Asp^{24}, $Tyr^{27}(SO_3)$, Nle^{28}, Gly^{29}, Gly^{29}, Trp^{30}, Nle^{31}, and Phe^{33} and receptor residues Glu^{345}, Arg^{197}, Leu^{199}, His^{347}, Leu^{348}, Leu^{99}, Phe^{107}, and Trp^{39}, respectively (Table 1). Twelve soft distance restraints based on fluorescence resonance energy transfer (FRET) data were set between the positions of Asp^{24}, Gly^{29}, and Phe^{33} of the CCK peptide and Cys^{94}, Asn^{102}, Ala^{204}, and Thr^{341} of the receptor (Table 2) (*30*). The peptide was first docked onto a grid representation of the receptor, followed by refinement. During refinement, the extracellular side of the transmembrane domain was represented by a full atomic model with a flexible side chain, while the rest of the

Table 2: $C_\alpha - C_\alpha$ Distances between Residues Labeled with a Fluorescence Group in the Best Models

CCK peptide residue	CCK receptor residue	β2-adrenergic receptor-based model (Å)	A2a-adenosine receptor-based model (Å)	FRET distance (*30*) (Å)
Aladan^{24}	Cys^{94}	26.1	24.6	21.7 ± 1.0
	N102C	18.1	19.5	16.5 ± 0.7
	A204C	19.2	26.3	24.5 ± 2.5
	T341C	14.7	17.3	15.9 ± 0.8
Aladan^{29}	Cys^{94}	20.1	21.1	22.7 ± 0.6
	N102C	12.4	16.4	16.5 ± 0.3
	A204C	16.5	17.2	21.0 ± 1.5
	T341C	17.0	16.8	16.3 ± 0.4
Aladan^{33}	Cys^{94}	23.9	21.7	21.2 ± 1.2
	N102C	13.4	14.2	15.9 ± 1.0
	A204C	21.2	23.0	25.8 ± 2.5
	T341C	20.9	20.0	15.8 ± 0.7

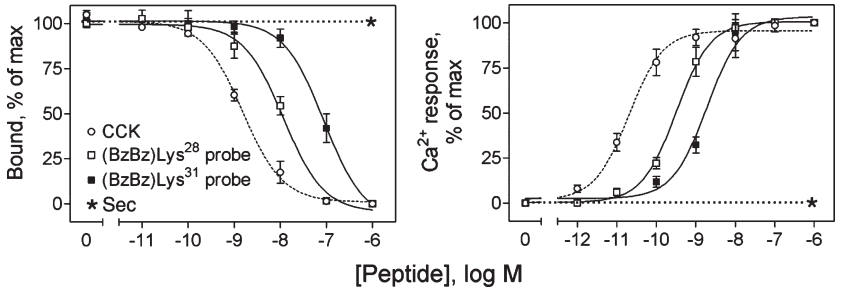

FIGURE 2: Functional characterization of the (BzBz)Lys^{28} and (BzBz)Lys^{31} probes. The left panel shows competition binding curves for CCK, secretin (Sec), and (BzBz)Lys^{28} and (BzBz)Lys^{31} probes competing for binding of ^{125}I-D-Tyr-Gly-[(Nle^{28,31})CCK-26−33] to CHO-CCKR membranes. Values represent percentages of maximal saturable binding that were observed in the absence of competitor. They are expressed as means ± the standard error of the mean of duplicate data from three independent experiments. The right panel shows intracellular calcium responses to increasing concentrations of the same peptides in CHO-CCKR cells. Basal levels of intracellular calcium were 150 ± 26 nM, and the maximal levels, similar for both probes and CCK, reached 389 ± 42 nM. Values are expressed as means ± the standard error of the mean of data from three independent experiments, with data normalized relative to the maximal response to CCK.

transmembrane domain was represented by grid maps. In addition, the backbone of extracellular loop 3 (ECL3), the portion of ECL2 in contact with the CCK peptide, and the top of transmembrane segment 1 (TM1) were allowed to be flexible, utilizing only a tether at both ends to maintain loop closure. All the variables of the peptide, backbone variables of the loops, and all side chain variables were progressively sampled. For each of the 100 independent runs, the best energy conformation was kept. These 100 conformations were further analyzed by ICM's energy function. The most reasonable conformations from each of the templates were selected for further modeling.

To extend the molecular model of the receptor to include its amino terminus, the NMR structure of the amino-terminal domain of the human CCK receptor was used to construct the first 37 residues of the rat CCK receptor (*29*). The carboxyl terminus of this domain was connected to the top of TM1. Thirty-three distance restraints were extracted from the original NMR study and imposed (*29*). The previously reported salt bridge between Asp^5 and Lys^{187} of the receptor (*31*) and the known disulfide linkage between Cys^{18} and Cys^{29} (*17*) were imposed. Three $Man_3GlcNAc_2$ pentasaccharides were attached to Asn^{10}, Asn^{24}, and Asn^{190} to mimic their N-linked glycosylation state. All the variables of the amino-terminal domain were sampled on a grid representation of the receptor transmembrane domain−CCK peptide complex, followed by energy minimization of the full atomic model. For each model from the two templates, 10 independent runs were attempted, and the best conformation in each series was selected as the final model. The two final models were evaluated with PROCHECK (*32*) and WHAT_CHECK (*33*).

RESULTS

Probe Characterization. Both the (BzBz)Lys^{28} and (BzBz)-Lys^{31} probes were synthesized by manual solid-phase techniques and purified by reversed-phase HPLC, and their identities were verified by mass spectrometry. They were functionally characterized in radioligand binding and biological activity assays. Figure 2 shows that both probes bound to the CCK receptor specifically and saturably, although with affinities lower than that of CCK [K_i values for CCK of 1.5 ± 0.1 nM, for the (BzBz)Lys^{28} probe of 11.7 ± 1.2 nM, and for the (BzBz)Lys^{31} probe of 88.0 ± 9.2 nM]. Figure 2 also shows that both probes were full agonists, stimulating intracellular calcium responses in a concentration-dependent manner, although they were less potent than natural CCK [EC_{50} values for CCK of 0.020 ± 0.003 nM, for the (BzBz)-Lys^{28} probe of 0.32 ± 0.08 nM, and for the (BzBz)Lys^{31} probe of 1.9 ± 0.2 nM]. Both probes also stimulated full intracellular calcium responses that were not different from those achieved in response to natural CCK (E_{max}, change from basal, 222 ± 20 nM). Structurally unrelated ligands, such as secretin, did not compete for binding of CCK radioligand to this preparation, nor did they elicit any intracellular calcium responses in CHO-CCKR cells (Figure 2).

Photoaffinity Labeling of the CCK Receptor. Both the (BzBz)Lys^{28} and (BzBz)Lys^{31} probes were tested for their ability

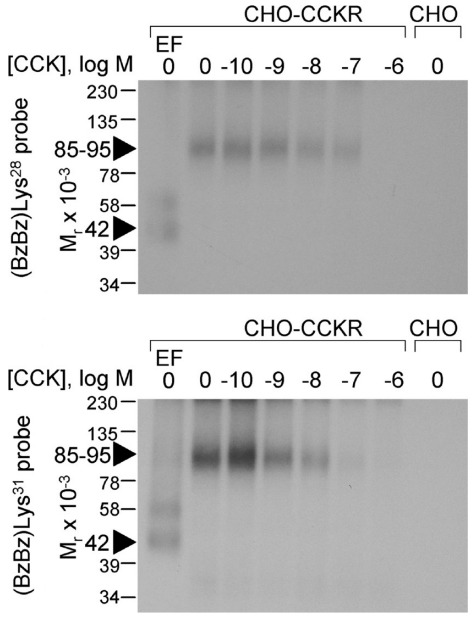

FIGURE 3: Photoaffinity labeling of the CCK receptor. Shown are typical autoradiographs of 10% SDS−polyacrylamide gel electrophoresis gels used to separate products of photoaffinity labeling of CHO-CCKR membranes with (BzBz)Lys^{28} (top) and (BzBz)Lys^{31} (bottom) probes in the absence and presence of increasing concentrations of competing unlabeled CCK. The CCK receptor labeled with each probe migrated similarly at an approximate M_r of 85000−95000 and shifted to an approximate M_r of 42000 after deglycosylation by endoglycosidase F (EF). The labeling by each probe was inhibited by CCK in a concentration-dependent manner. No band was detected in affinity-labeled non-receptor-bearing CHO cell membranes. This pattern is representative of three independent experiments.

to covalently label the CCK receptor. Figure 3 shows that they both labeled the CCK receptor specifically and saturably, with CCK competing for this labeling in a concentration-dependent manner. The labeled receptor bands migrated at an approximate M_r of 85000−95000 and shifted to an approximate M_r of 42000 after deglycosylation with endoglycosidase F. No radioactive band was observed in the affinity-labeled non-receptor-bearing CHO cell membranes.

Labeling Site Identification. CNBr cleavage was used as the first indication as the region of labeling for each probe. Theoretically, CNBr cleavage of the CCK receptor would yield 16 peptide fragments ranging in molecular mass from 0.1 to 9.9 kDa, two of which contain potential sites of N-linked glycosylation (Figure 4). Figure 4 shows that CNBr cleavage of the CCK receptor labeled with the (BzBz)Lys^{28} probe resulted in a nonglycosylated fragment migrating at an approximate M_r of 2500−3500. Similarly, CNBr cleavage of the CCK receptor labeled with the (BzBz)Lys^{31} probe also yielded a small nonglycosylated fragment that migrated at an approximate M_r of 3500−4500. The nonglycosylated nature of the labeled peptide ruled out the labeling of the amino-terminal fragment (Asn^{10}−Met^{72}) of the receptor, which is known to be glycosylated (*11*). Considering the mass of the attached probe (1536 for both probes), we would expect the candidate fragment to be in the range of 1−2 kDa for the (BzBz)Lys^{28} probe and 2−3 kDa for the (BzBz)Lys^{31} probe. This suggests that the first and second extracellular loops (ECL1 and ECL2, respectively) were the most likely to represent the labeled regions of the receptor for both probes. However, small peptides often do not migrate true to their masses, and different standards can migrate differently in this range. Therefore, no fragment from any of the three extracellular loops could be excluded at this stage as a candidate for representing the regions of labeling.

To further identify which fragment contained the region of labeling for each of the probes, three receptor mutants were used in which either an additional Met residue was introduced (L104M in ECL1 or V342M in ECL3) or a naturally occurring Met residue was eliminated (M195L in ECL2) from each of the three extracellular loop regions. These receptor constructs were well characterized as having binding and biological activities similar to those of the wild-type CCK receptor (*7*, *10*, *16*). Each of these constructs was specifically and saturably labeled by each probe (data not shown).

Figure 5 shows that for the (BzBz)Lys^{28} probe, CNBr cleavage of the labeled M195L receptor mutant resulted in a radioactive band migrating at an approximate M_r of 4500−5500, clearly distinct from that of the CNBr fragments from the wild-type, L104M, and V342M CCK receptors (M_r = 2500−3500), indicating that the fragment spanning ECL2 (Thr^{174}−Met^{205}) contained the site of labeling for the (BzBz)Lys^{28} probe. For the (BzBz)Lys^{31} probe, CNBr cleavage of the labeled L104M mutant receptor resulted in a radioactive band migrating at an approximate M_r of 2500−3500, clearly distinct from that of the CNBr cleavage products from the wild-type, M195L, and V342M CCK receptors (M_r = 3500−4500). This indicates that the fragment spanning ECL1 (Pro^{96}−Met^{121}) contained the site of labeling for the (BzBz)Lys^{31} probe.

To determine whether the amino-terminal half (Thr^{174}−Met^{195}) or the carboxyl-terminal half (Cys^{196}−Met^{205}) of the ECL2 fragment contained the site of labeling for the (BzBz)Lys^{28} probe, the labeled peptide from CNBr cleavage of the wild-type receptor was further cleaved with endoproteinase Lys-C. Figure 6 shows that treatment with this protease did not change the migration of the labeled CNBr fragment, suggesting that the carboxyl-terminal segment of the ECL2 fragment (Cys^{196}−Met^{205}) represented the region of labeling by this probe. This was confirmed by CNBr cleavage of the M205L mutant receptor in which a naturally occurring Met residue in ECL2 was eliminated. Figure 7 shows that the M205L mutant receptor bound CCK and signaled normally and was able to be labeled by the (BzBz)Lys^{28} probe. CNBr cleavage of the labeled M205L mutant receptor yielded a labeled band migrating at an approximate M_r of 4500−5500, clearly distinct from that derived from cleavage of the wild-type receptor (M_r = 2500−3500). This provided definitive identification of the Cys^{196}−Met^{205} segment as the region of labeling with the (BzBz)Lys^{28} probe.

The specific receptor residue labeled by the (BzBz)Lys^{28} probe was identified by radiochemical sequencing of the Cys^{196}−Met^{205} fragment derived from CNBr cleavage of the labeled A204C mutant receptor. This mutant receptor was specifically and saturably labeled by the (BzBz)Lys^{28} probe (data not shown), and the Cys^{196}−Met^{205} fragment from CNBr cleavage of the A204C receptor was purified to radiochemical homogeneity and coupled to *N*-(2-aminoethyl-1)-3-aminopropyl glass beads through Cys^{204} for manual Edman degradation sequencing. Figure 8 shows the profile of eluted radioactivity in which a peak was found in cycle 4. This identified Leu^{199} of the CCK receptor as the site of labeling by the (BzBz)Lys^{28} probe.

To identify the specific receptor residue labeled by the (BzBz)-Lys^{31} probe, radiochemical sequencing of the CNBr fragments from both the labeled wild-type and L104M mutant receptors was performed. As shown in Figure 8, a radioactive peak eluted

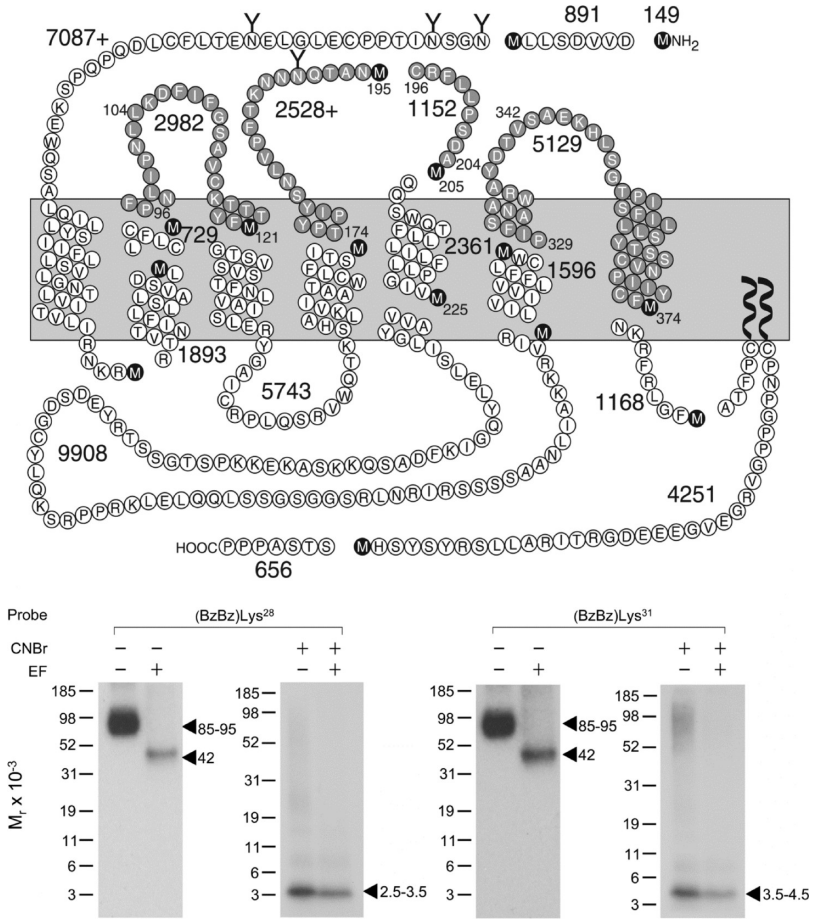

FIGURE 4: CNBr cleavage of the CCK receptor labeled with the (BzBz)Lys^{28} and (BzBz)Lys^{31} probes. The top panel is a diagram of the predicted sites of CNBr cleavage of the CCK receptor, noting the sites of N-linked glycosylation. The bottom panel shows typical autoradiographs of 10% NuPAGE gels used to separate the native and deglycosylated CCK receptor that had been labeled with each of the probes and the products of subsequent CNBr cleavage. CNBr cleavage of the CCK receptor labeled with the (BzBz)Lys^{28} and (BzBz)Lys^{31} probes each yielded a labeled fragment migrating at an approximate M_r of 2500−3500 and 3500−4500, respectively. The migration of neither fragment was affected by treatment with endoglycosidase F (EF). This pattern is representative of at least 10 independent experiments. Fragments spanning the three extracellular loops (highlighted in gray) are all possible candidates for representing the regions of labeling by both of the probes.

in cycle 3 when the Lys^{105}−Met^{121} fragment was sequenced from the labeled L104M mutant, whereas no peak was found when the Pro^{96}−Met^{121} fragment was sequenced from the labeled wild-type receptor. This indicated that the probe specifically labeled residue Phe^{107} of the CCK receptor.

Molecular Modeling. We have used the recently published crystal structures of the human β2-adrenergic receptor and the A2a-adenosine receptor, which have higher degrees of sequence similarity and, therefore, may represent better templates than rhodopsin, to generate the current homology models of the CCK receptor (*1*, *2*). The two templates were used in two independent simulations. In each simulation, the extracellular loops were thoroughly sampled and 100 diverse loop conformations were used as starting points for peptide docking. Eight distance restraints obtained from photoaffinity labeling studies and 12 soft restraints from FRET studies were imposed on the model to guide the peptide docking simulation (*30*). We have selected the best model from each template on the basis of ICM's global energetics. The models were further evaluated with PROCHECK and WHAT_CHECK, both having >97% backbone dihedrals in the allowed regions and a second generation packing quality of greater than −0.6. The final peptide docking poses of the best model from each of the two templates were remarkably similar to each other, and quite distinct from that previously generated using rhodopsin as a template (Figure 9). Table 1 lists the C_β−C_β distances between cross-linked residues. Note that all distances were well within the reach of a photolabile group. The salt bridge between CCK peptide residue Tyr^{27}(SO_3) and receptor residue Arg^{197} was well-preserved in these models. Table 2 lists the C_α−C_α distances between residues decorated with fluorescent moieties in the FRET studies. The fluorescent group is attached to its receptor residues via a flexible linker (*30*, *34*), so the C_α−C_α distances can give us only a general idea of the actual distances between the natural amino acid residues in those positions. Nevertheless, the C_α−C_α distances are in general agreement with the experimental data.

In both of the new homology models, the CCK peptide-binding pocket was defined by the top of TM2, ECL2, ECL3, and TM7. The amino terminus of CCK-26−33 binds near the top of ECL3, fully compatible with docking of the longer CCK peptides with additional residues extending beyond this point. The mid-region of CCK-26−33 is in close contact with the binding pocket, with its hydrophobic Nle^{28} and Nle^{31} (Met residues in natural CCK) in close contact with Leu^{199} and Phe^{107} of the receptor, and with Tyr^{27}(SO_3) forming an essential salt bridge with Arg^{197}. The carboxyl terminus of CCK-26−33 is then situated between the top of TM1 and TM7, with Phe^{33} being in the proximity of Trp^{39} near the top of TM1. It is noteworthy that the amino terminus of

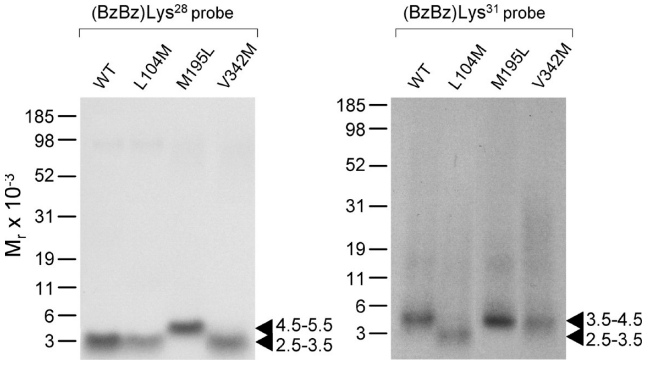

FIGURE 5: Autoradiographs of products of CNBr cleavage of the L104M, M195L, and V342M mutant CCK receptors labeled with the (BzBz)Lys^{28} and (BzBz)Lys^{31} probes. In the left panel, CNBr cleavage of the M195L mutant receptor labeled with the (BzBz)Lys^{28} probe yielded a fragment migrating at an approximate M_r of 4500−5500, which was distinct from the M_r = 2500−3500 fragment that resulted from the cleavage of the wild-type, L104M, and V342M receptors labeled with the same probe. This indicates that the Thr^{174}−Met^{205} fragment (see the diagram in Figure 4) spanning ECL2 contained the region of labeling with the (BzBz)Lys^{28} probe. In the right panel, CNBr cleavage of the L104M mutant receptor labeled with the (BzBz)Lys^{31} probe yielded a fragment migrating at an approximate M_r of 2500−3500, which was distinct from the M_r = 3500−4500 fragment that resulted from cleavage of the wild-type, L104M, and V342M receptors labeled with the same probe. This indicates that the Pro^{96}−Met^{121} fragment (see the diagram in Figure 4) spanning ECL1 contained the site of labeling with the (BzBz)Lys^{31} probe. This pattern is representative of three independent experiments.

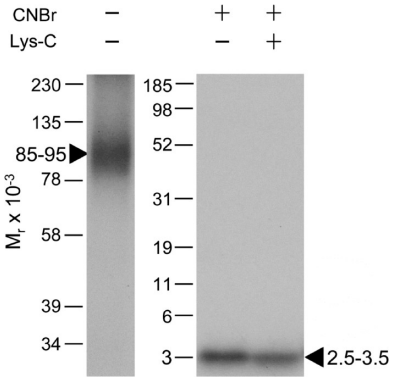

FIGURE 6: Autoradiographs reflecting sequential endoproteinase Lys-C cleavage of the CNBr fragment of the CCK receptor labeled with the (BzBz)Lys^{28} probe. Further endoproteinase Lys-C cleavage of the labeled CNBr fragment from the wild-type CCK receptor did not change its migration on a 10% NuPAGE gel, suggesting that the site of labeling was within the smaller non-lysine-containing carboxyl-terminal Cys^{196}−Met^{205} segment (see the diagram in Figure 4) in ECL2. These data are representative of results from three independent experiments. This was confirmed by CNBr cleavage of the M205L mutant receptor in Figure 7. Also shown is a representative autoradiograph of the CCK receptor labeled with the same probe run on a 10% SDS−polyacrylamide gel prior to these cleavage steps.

the CCK peptide moves out of the binding pocket and can easily be extended, as it is in the various longer molecular forms of this hormone, without contacting or interfering with any portion of the receptor. A more detailed view of the β2-adrenergic receptor-based model is shown in Figure 10 and is demonstrated to be fully compatible with all the experimental data generated to date.

We have also completed this full model by rebuilding the amino-terminal end of the rat CCK receptor using the NMR model of this region of the human CCK receptor as a starting

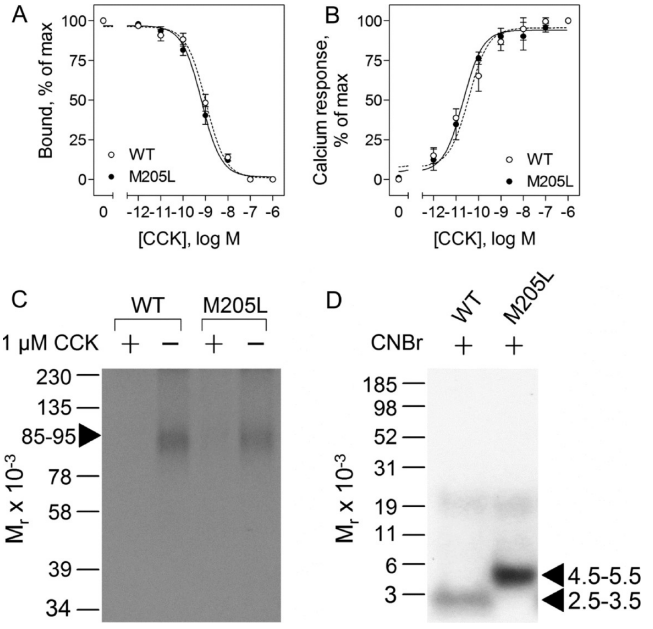

FIGURE 7: Confirmation of the domain of labeling for the (BzBz)-Lys^{28} probe by CNBr cleavage of the M205L mutant receptor. Shown are CCK competition binding data (A) and concentration−response data for CCK-stimulated intracellular calcium (B) for wild-type and M205L CCK receptor constructs transiently expressed in COS-1 cells. Basal levels of intracellular calcium were 148 ± 19 nM, with the maximal stimulated levels reaching 255 ± 29 nM. Values represent means ± the standard error of the mean of data from a minimum of three independent experiments performed in duplicate. Shown also are representative autoradiographs of the saturable photoaffinity labeling by the (BzBz)Lys^{28} probe (C) and CNBr cleavage (D) of the wild-type and mutant CCK receptor constructs transiently expressed in COS-1 cells. Like in CHO cells, CNBr cleavage of the wild-type CCK receptor expressed in COS-1 cells yielded a labeled band migrating at an approximate M_r of 2500−3500. This band shifted to an approximate M_r of 4500−5500 in the M205L CCK receptor, indicating that the site of labeling was between Cys^{196} and Met^{205}. Data are representative of three independent experiments.

point (*29*). We were able to obtain only 33 distance restraints from the original NMR study, while 165 internal variables are needed to fully define this region, highlighting its underdefined nature. The intradomain disulfide bond between Cys^{18} and Cys^{29} (*17*) and the previously reported salt bridge between receptor residues Asp^{5} and Lys^{187} (*31*) helped limit the conformational space that was sampled. The best models demonstrated that the amino-terminal domain partially covers CCK-26−33, partially shielding the Tyr^{27}(SO_3)−Arg^{197} salt bridge from solvation, while leaving the amino-terminal end of CCK-26−33 accessible for peptide extension in its longer molecular forms (Figure 10, bottom panel). However, the highly underdefined nature of this amino-terminal region of the receptor prevents further meaningful residue−residue approximation predictions for this region.

DISCUSSION

A detailed understanding of the molecular basis of ligand binding and activation of a receptor provides key information that can be useful in the development and refinement of receptor-active drugs. The recent solution of the high-resolution crystal structures of the β2-adrenergic receptor and A2a-adenosine receptor has provided two very useful templates for GPCRs in family A (*1*, *2*). Both structures were as different from the

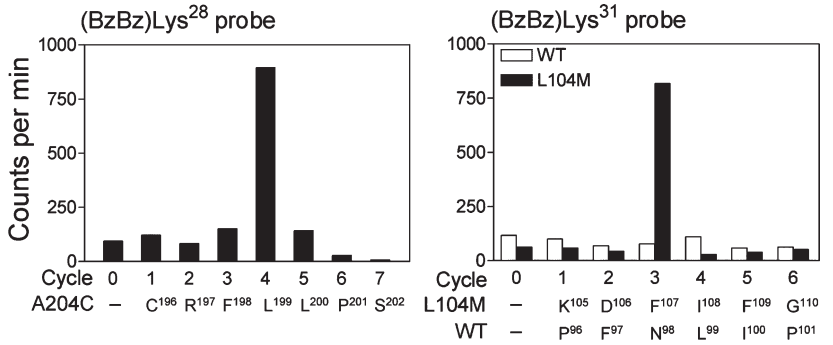

FIGURE 8: Identification of the labeled receptor residues. The left panel shows a representative radioactive elution profile from Edman degradation sequencing of the purified CNBr fragment (Cys^{196}–Met^{205}) of the A204C mutant CCK receptor labeled with the (BzBz)Lys^{28} probe. The peak in eluted radioactivity was observed in cycle 4, corresponding to covalent attachment of peptide probe residue (BzBz)Lys^{28} to receptor residue Leu^{199}. The right panel shows a representative radioactive elution profile from sequencing of the purified CNBr fragments, Pro^{96}–Met^{121} of the wild type and Lys^{105}–Met^{121} of the L104M mutant CCK receptor labeled with the (BzBz)Lys^{31} probe. A peak in radioactivity occurred in elution cycle 3 for the L104M mutant receptor, representing covalent labeling of receptor residue Phe^{107} by the (BzBz)-Lys^{31} probe. No peak was observed in six cycles of sequencing of the CNBr fragment from the wild-type CCK receptor (WT) labeled with the same probe. These data are representative of three independent experiments.

previous best structure for a receptor in this family, rhodopsin, as the structure of rhodopsin had been different from the structure of bacteriorhodopsin, the previous best template (*6*). While these models are clearly improving for the prediction of structures of other classical GPCRs in this family, a detailed molecular understanding of the basis of ligand binding to them is largely limited to the GPCRs that are naturally activated by small molecules that act within the relatively constrained helical bundle domain. In contrast, peptides are believed to bind predominantly to extracellular loop and tail domains of their receptors (*35*). These regions of the receptors are much less well conserved and are likely quite varied in structure from one receptor to another. This creates major challenges for meaningful insights into the molecular basis of binding and activation of such receptors by peptide ligands.

The purpose of this work was to enhance our understanding of the molecular basis of binding and activation of a peptide hormone receptor in this family, the type 1 (or type A) CCK receptor. This is a receptor that plays important roles in nutrient homeostasis. It is present in the pancreas, gallbladder, gastrointestinal smooth muscle and nerves, and specific brain nuclei, where it acts to stimulate pancreatic exocrine secretion, gallbladder emptying, enteric motility, and postcibal satiety (*36*). To achieve these insights, we have developed two homology models for this receptor, one based on the β2-adrenergic receptor structure and another based on the A2a-adeonsine receptor structure, and we have utilized a broad variety of experimentally derived constraints to refine these models. This includes the development, characterization, and application of two new intrinsic photoaffinity labeling probes, increasing the number of spatial approximation constraints to seven. It is noteworthy that these experimentally derived constraints were all generated with full agonist analogues of the natural peptide ligand, and that this included sites of covalent attachment in six of seven residues within its highly focused pharmacophoric domain.

On the basis of these data, the site of docking of CCK in molecular modeling approaches was highly consistent and converged quite nicely from the two distinct templates. CCK was found to bind at the extracellular surface and above the lipid bilayer to a pocket defined by the top of transmembrane segment 2, extracellular loops 2 and 3, and the top of transmembrane segment 7. The carboxyl terminus of CCK in this model is located above the helical bundle. This is generally consistent with the previously described model that was based on a smaller number of photoaffinity labeling constraints and the rhodopsin homology template (*8*). It is, however, quite distinct from the alternative model that was based largely on mutagenesis data (*12*). As in both previous molecular models, the functionally important acidic tyrosine sulfate moiety within CCK in the current model is found to form a complex nicely with the basic Arg^{197} in extracellular loop 2.

This site of peptide docking with the CCK receptor in the current refined molecular model was also consistent with 12 measurements coming from FRET experiments with distances from each of three positions distributed throughout the CCK peptide to each of four positions in the ectodomain of the CCK receptor (*30*). These data nicely support the docked pose of CCK with its carboxyl terminus close to Asn^{102} near the top of transmembrane segment 2, with its midregion closest to Ala^{204} in extracellular loop 2 and Thr^{341} near the top of transmembrane segment 6. In contrast, the alternative model that came largely from indirect mutational studies in which the amino terminus of CCK resides closest to the top of transmembrane segment 1 and the carboxyl terminus resides closest to the top of transmembrane segment 6 is inconsistent with these FRET data.

The models currently being proposed are also consistent with everything we know from existing peptide and receptor structure–activity studies. Key is the ability of this model to accommodate the various extended molecular forms of CCK, with the amino terminus of CCK-26–33 residing in a position that would easily allow peptide extension without interference with any important structures. Similarly, the sites of glycosylation are fully accommodated by this model, all situated directly out and away from any site of peptide docking or any other important structure. The functionally important salt bridge postulated to exist between acidic tyrosine sulfate at position 27 of CCK and the basic Arg^{197} residue within receptor extracellular loop 2 (*37*) is partially shielded from solvation by the amino terminus of the receptor, as this is positioned in the current models.

Indeed, the current models provide substantial enhancements from that previously proposed that was based on the rhodopsin structure. Both models originating from the homology structure based on the β2-adrenergic receptor and the A2a-adenosine receptor positioned the docked peptide above the second

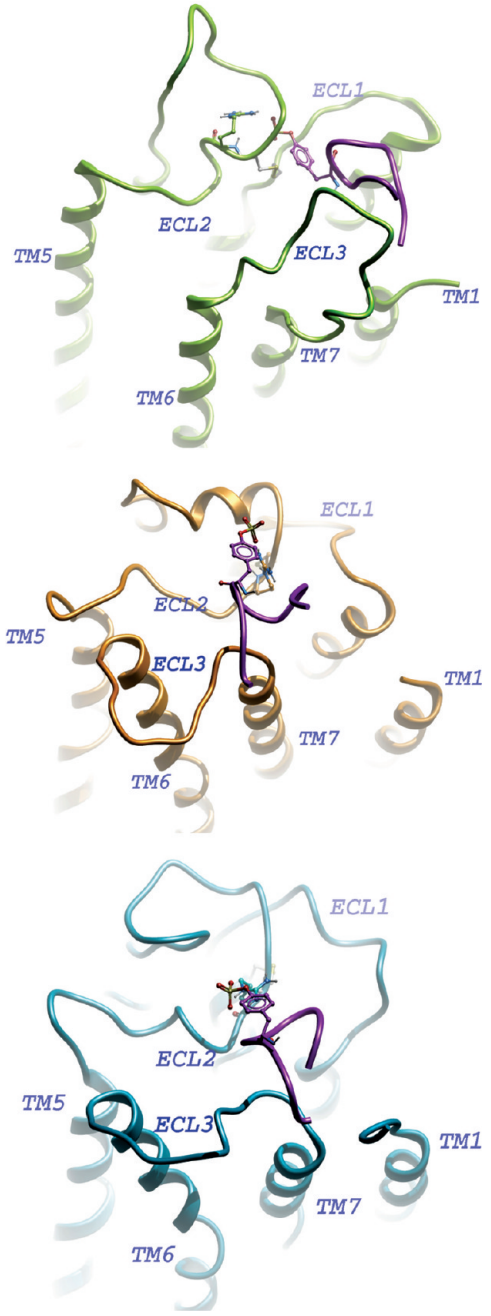

FIGURE 9: Molecular models of the CCK-occupied CCK receptor. Shown are views of the best molecular models of CCK-24−33 occupying the CCK receptor that are based on rhodopsin (green, top), the β2-adrenergic receptor (orange, middle), and the A2a-adenosine receptor (cyan, bottom). In each model, the ligand is colored magenta. All three models are viewed from the same angle of perspective for easy comparison. The salt bridge between the acidic tyrosine sulfate in position 27 of CCK and the basic Arg^{197} residue within receptor extracellular loop 2 is expanded in each model.

extracellular loop, forming the essential salt bridge in that region. In contrast, in the previous model based on the rhodopsin structure, the peptide was situated closer to the second and third helices, forming the salt bridge behind the second extracellular loop on top of the third helix. The convergence from quite distinct starting structures to yield a consistent mode of peptide docking in the two current models provides strong support for the validity of this new insight. This provides the highest level of refinement yet available to demonstrate the docking of a peptide hormone to a family A GPCR.

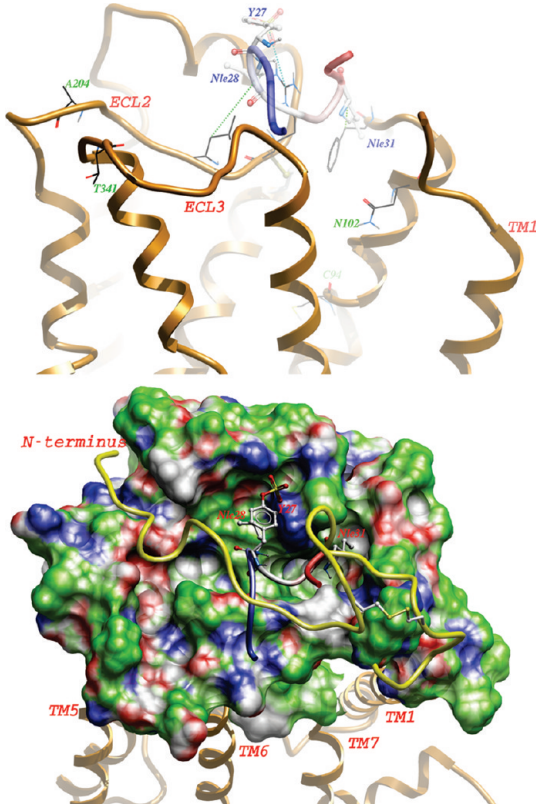

FIGURE 10: Key characteristics of the molecular model of the CCK-occupied CCK receptor. Shown are views of the best current three-dimensional molecular model of the CCK-occupied CCK receptor (based on homology with the structure of the β2-adrenergic receptor) that incorporated all extant photoaffinity labeling spatial approximation constraints, FRET distance constraints, and experimentally derived disulfide bonds and salt bridges, as well as insights coming from structure−activity studies. The CCK peptide ligand is colored from blue to red from the amino terminus to carboxyl terminus, respectively, with residues labeled in blue. The receptor backbone is colored tan, with domains labeled in red and receptor positions utilized in the FRET studies labeled in green. Key residues have been expanded, with their targets of covalent labeling in photoaffinity labeling studies connected by green dotted lines. The top model (lateral view) is best developed and fully supported by these data, while the bottom model (top view) is similar, with the addition of the receptor amino-terminal domain (backbone colored yellow) with its conformation less well constrained by existing experimental data. In the bottom model, two pairs of salt bridges between receptor residues Asp^{5} and Lys^{187} and between CCK peptide residue Tyr^{27} and receptor residue Arg^{197} have helped to orient the amino terminus relative to the body of the receptor. In the bottom model, the peptide-binding surface on the top of the transmembrane helical bundle domain is shown with component residues color coded (green for hydrophobic surface, blue for positively charged, and red for negatively charged). TM, transmembrane segment; ECL, extracellular loop; N-terminus, amino terminus.

ACKNOWLEDGMENT

We acknowledge contributions to this work by Dr. X.-Q. Ding, who performed some of the earliest studies with these probes, and Dr. F. Gao, who helped with early molecular modeling studies.

REFERENCES

1. Cherezov, V., Rosenbaum, D. M., Hanson, M. A., Rasmussen, S. G., Thian, F. S., Kobilka, T. S., Choi, H. J., Kuhn, P., Weis, W. I., Kobilka, B. K., and Stevens, R. C. (2007) High-resolution crystal structure of an engineered human β2-adrenergic G protein-coupled receptor. *Science 318*, 1258–1265.

2. Jaakola, V. P., Griffith, M. T., Hanson, M. A., Cherezov, V., Chien, E. Y., Lane, J. R., Ijzerman, A. P., and Stevens, R. C. (2008) The 2.6 angstrom crystal structure of a human A2A adenosine receptor bound to an antagonist. *Science 322*, 1211–1217.
3. Scheerer, P., Park, J. H., Hildebrand, P. W., Kim, Y. J., Krauss, N., Choe, H. W., Hofmann, K. P., and Ernst, O. P. (2008) Crystal structure of opsin in its G-protein-interacting conformation. *Nature 455*, 497–502.
4. Warne, T., Serrano-Vega, M. J., Baker, J. G., Moukhametzianov, R., Edwards, P. C., Henderson, R., Leslie, A. G., Tate, C. G., and Schertler, G. F. (2008) Structure of a β1-adrenergic G-protein-coupled receptor. *Nature 454*, 486–491.
5. Miller, L. J., and Gao, F. (2008) Structural basis of cholecystokinin receptor binding and regulation. *Pharmacol. Ther. 119*, 83–95.
6. Palczewski, K., Kumasaka, T., Hori, T., Behnke, C. A., Motoshima, H., Fox, B. A., Le Trong, I., Teller, D. C., Okada, T., Stenkamp, R. E., Yamamoto, M., and Miyano, M. (2000) Crystal structure of rhodopsin: A G protein-coupled receptor. *Science 289*, 739–745.
7. Arlander, S. J., Dong, M., Ding, X. Q., Pinon, D. I., and Miller, L. J. (2004) Key differences in molecular complexes of the cholecystokinin receptor with structurally related peptide agonist, partial agonist, and antagonist. *Mol. Pharmacol. 66*, 545–552.
8. Ding, X. Q., Dolu, V., Hadac, E. M., Holicky, E. L., Pinon, D. I., Lybrand, T. P., and Miller, L. J. (2001) Refinement of the structure of the ligand-occupied cholecystokinin receptor using a photolabile amino-terminal probe. *J. Biol. Chem. 276*, 4236–4244.
9. Dong, M., Hadac, E. M., Pinon, D. I., and Miller, L. J. (2005) Differential spatial approximation between cholecystokinin residue 30 and receptor residues in active and inactive conformations. *Mol. Pharmacol. 67*, 1892–1900.
10. Hadac, E. M., Pinon, D. I., Ji, Z., Holicky, E. L., Henne, R. M., Lybrand, T. P., and Miller, L. J. (1998) Direct identification of a second distinct site of contact between cholecystokinin and its receptor. *J. Biol. Chem. 273*, 12988–12993.
11. Ji, Z., Hadac, E. M., Henne, R. M., Patel, S. A., Lybrand, T. P., and Miller, L. J. (1997) Direct identification of a distinct site of interaction between the carboxyl-terminal residue of cholecystokinin and the type A cholecystokinin receptor using photoaffinity labeling. *J. Biol. Chem. 272*, 24393–24401.
12. Archer-Lahlou, E., Tikhonova, I., Escrieut, C., Dufresne, M., Seva, C., Pradayrol, L., Moroder, L., Maigret, B., and Fourmy, D. (2005) Modeled structure of a G-protein-coupled receptor: The cholecystokinin-1 receptor. *J. Med. Chem. 48*, 180–191.
13. Pearson, R. K., Miller, L. J., Hadac, E. M., and Powers, S. P. (1987) Analysis of the carbohydrate composition of the pancreatic plasmalemmal glycoprotein affinity labeled by short probes for the cholecystokinin receptor. *J. Biol. Chem. 262*, 13850–13856.
14. Powers, S. P., Pinon, D. I., and Miller, L. J. (1988) Use of N,O-bis-Fmoc-D-Tyr-ONSu for introduction of an oxidative iodination site into cholecystokinin family peptides. *Int. J. Pept. Protein Res. 31*, 429–434.
15. Hadac, E. M., Ghanekar, D. V., Holicky, E. L., Pinon, D. I., Dougherty, R. W., and Miller, L. J. (1996) Relationship between native and recombinant cholecystokinin receptors: Role of differential glycosylation. *Pancreas 13*, 130–139.
16. Gigoux, V., Escrieut, C., Silvente-Poirot, S., Maigret, B., Gouilleux, L., Fehrentz, J. A., Gully, D., Moroder, L., Vaysse, N., and Fourmy, D. (1998) Met-195 of the cholecystokinin-A receptor interacts with the sulfated tyrosine of cholecystokinin and is crucial for receptor transition to high affinity state. *J. Biol. Chem. 273*, 14380–14386.
17. Ding, X. Q., Dolu, V., Hadac, E. M., Schuetz, M., and Miller, L. J. (2003) Disulfide bond structure and accessibility of cysteines in the ectodomain of the cholecystokinin receptor: Specific mono-reactive receptor constructs examine charge-sensitivity of loop regions. *Receptors Channels 9*, 83–91.
18. Holtmann, M. H., Ganguli, S., Hadac, E. M., Dolu, V., and Miller, L. J. (1996) Multiple extracellular loop domains contribute critical determinants for agonist binding and activation of the secretin receptor. *J. Biol. Chem. 271*, 14944–14949.
19. Munson, P. J., and Rodbard, D. (1980) Ligand: A versatile computerized approach for characterization of ligand-binding systems. *Anal. Biochem. 107*, 220–239.
20. Grynkiewicz, G., Poenie, M., and Tsien, R. Y. (1985) A new generation of Ca^{2+} indicators with greatly improved fluorescence properties. *J. Biol. Chem. 260*, 3440–3450.
21. Laemmli, U. K. (1970) Cleavage of structural proteins during the assembly of the head of bacteriophage T4. *Nature 227*, 680–685.
22. Dong, M., Wang, Y., Pinon, D. I., Hadac, E. M., and Miller, L. J. (1999) Demonstration of a direct interaction between residue 22 in the carboxyl-terminal half of secretin and the amino-terminal tail of the secretin receptor using photoaffinity labeling. *J. Biol. Chem. 274*, 903–909.
23. Dong, M., Wang, Y., Hadac, E. M., Pinon, D. I., Holicky, E., and Miller, L. J. (1999) Identification of an interaction between residue 6 of the natural peptide ligand and a distinct residue within the amino-terminal tail of the secretin receptor. *J. Biol. Chem. 274*, 19161–19167.
24. Abagyan, R., Totrov, M., and Kuznetsov, D. (1994) ICM: A new method for protein modeling and design: Applications to docking and structure prediction from the distorted native confirmation. *J. Comput. Chem. 15*, 488–506.
25. Abagyan, R., and Totrov, M. (1994) Biased probability Monte Carlo conformational searches and electrostatic calculations for peptides and proteins. *J. Mol. Biol. 235*, 983–1002.
26. Metropolis, N., Rosenbluth, A. W., Rosenbluth, M. N., Teller, A. H., and Teller, E. (1953) Equation of State Calculations by Fast Computing Machines. *J. Chem. Phys. 21*, 1087–1092.
27. Hulo, N., Bairoch, A., Bulliard, V., Cerutti, L., Cuche, B. A., de Castro, E., Lachaize, C., Langendijk-Genevaux, P. S., and Sigrist, C. J. (2008) The 20 years of PROSITE. *Nucleic Acids Res. 36*, D245–D249.
28. Dong, M., Lam, P. C., Pinon, D. I., Sexton, P. M., Abagyan, R., and Miller, L. J. (2008) Spatial approximation between secretin residue five and the third extracellular loop of its receptor provides new insight into the molecular basis of natural agonist binding. *Mol. Pharmacol. 74*, 413–422.
29. Pellegrini, M., and Mierke, D. F. (1999) Molecular complex of cholecystokinin-8 and N-terminus of the cholecystokinin A receptor by NMR spectroscopy. *Biochemistry 38*, 14775–14783.
30. Harikumar, K. G., Gao, F., Pinon, D. I., and Miller, L. J. (2008) Use of multidimensional fluorescence resonance energy transfer to establish the orientation of cholecystokinin docked at the type A cholecystokinin receptor. *Biochemistry 47*, 9574–9581.
31. Dong, M., Ding, X. Q., Thomas, S. E., Gao, F., Lam, P. C., Abagyan, R., and Miller, L. J. (2007) Role of lysine187 within the second extracellular loop of the type A cholecystokinin receptor in agonist-induced activation. Use of complementary charge-reversal mutagenesis to define a functionally important interdomain interaction. *Biochemistry 46*, 4522–4531.
32. Laskowski, R. A., Macarthur, M. W., Moss, D. S., and Thornton, J. M. (1993) Procheck: A Program to Check the Stereochemical Quality of Protein Structures. *J. Appl. Crystallogr. 26*, 283–291.
33. Hooft, R. W. W., Vriend, G., Sander, C., and Abola, E. E. (1996) Errors in protein structures. *Nature 381*, 272–272.
34. Harikumar, K. G., Pinon, D. I., and Miller, L. J. (2006) Fluorescent indicators distributed throughout the pharmacophore of cholecystokinin provide insights into distinct modes of binding and activation of type A and B cholecystokinin receptors. *J. Biol. Chem. 281*, 27072–27080.
35. Ji, T. H., Grossmann, M., and Ji, I. (1998) G protein-coupled receptors. I. Diversity of receptor-ligand interactions. *J. Biol. Chem. 273*, 17299–17302.
36. Liddle, R. A. (1994) Cholecystokinin. In *Gut Peptides: Biochemistry and Physiology* (Walsh, J. H., and Dockray, G. J., Eds.) pp 175−216, Raven Press, New York.
37. Ding, X. Q., Pinon, D. I., Furse, K. E., Lybrand, T. P., and Miller, L. J. (2002) Refinement of the conformation of a critical region of charge-charge interaction between cholecystokinin and its receptor. *Mol. Pharmacol. 61*, 1041–1052.